Transport model of thermal and epithermal positrons in solids. I

Y. Kong* and K. G. Lynn
Department of Physics, Brookhaven National Laboratory, Upton, New York 11973
(Received 15 March 1989)

Epithermal positron transport in solids is treated by employing a one-dimensional Boltzmann equation, which, in combination with the diffusion equation for the thermalized positrons, gives rise to a more realistic model for transport of positrons implanted into solids with variable energies. Thermalization is accounted for by the averaged inelastic scattering of the epithermal positrons, although the epithermal positron energy distribution cannot be predicted from this model.

I. INTRODUCTION

Variable-energy positron beams have been utilized for studying various aspects of the properties of solids in recent years.[1] After positrons are implanted into the solids and experience energy degradation, an implantation profile is usually assumed for the "stopped" positrons,[2] and their subsequent transport is described by a diffusion equation.[3] Although this picture has yielded a lot of information on positron transport characteristics as well as material defects distributions, there have been some difficulties in understanding the experimental results. For example, the temperature dependence of the diffusion coefficient of several metals has been found to contradict the prediction of $T^{-1/2}$ behavior.[4] Huomo *et al.* have suggested that the deviation is associated with the nonthermal positrons.[5] In their data analysis, the low-energy spectrum is neglected, with the high-energy data giving reasonable agreement with the $T^{-1/2}$ behavior. Another example is the total reflection of thermalized positrons as $T \rightarrow 0$ K predicted by Nieminen and Oliva.[6] Initial experiments carried out at Brookhaven found disagreement with this prediction,[7,8] but recently, the experiment of Britton *et al.*[9] has indicated that quantum reflection at low temperature does occur. The question naturally arises as to whether the inconsistency is fully attributable to the nonthermal positrons. Other explanations, such as inelastic processes at the surface,[10] have also been suggested.

Theoretically, the direct employment of a diffusion equation for the implanted positrons is inappropriate in that the thermalization is not correctly treated. When fitting the diffusion equation to the experimental data, the measured signal will actually be a mixture of positron thermalization and transport effects, so it is necessary to develop a model that will take into account the nonthermal positrons and their thermalization. This kind of model will help distinguish between the contributions of thermal and epithermal positrons to the detected signal.

In other experimental efforts, epithermal positrons have been discussed in the context of probing near surface trapping centers,[11] reemitted positron energy spectra from ionic solids,[12] and rare-gas solids,[13] as well as Ps formation by picking up electrons at the surface by the back-diffused epithermal positrons.[14] These and some recent developments of variable energy positron beams probing multilayered structures also give rise to the need to be able to take into account the epithermal positrons. Experiments on thin metal overlayers,[15] where the positron experiences an acceleration by the interfacial dipole and are not treatable by the ordinary diffusion model for thermal positrons have been performed. We have extended our present model to the reemission fraction of epithermal positrons for a bilayer system. The results are planned to be presented elsewhere.[16]

Previous efforts in modeling the epithermal positrons have not been satisfactory. Howell *et al.*[14] scaled the available data for electron total backscattering in order to fit their nonthermal positronium measurement, which yielded a E^{-1} dependence of the positronium intensity on the incident positron energy. Another approach by Britton *et al.*[17] is inappropriate in several respects; for example, elastic scattering with mean free path (mfp) 20 Å is used to characterize the escape depth of epithermal positrons, while we characterize this length as the thermalization length, which is more related to the inelastic mean free path. Further, the depletion of the reemitted thermal fraction at low energies because of the epithermal positron's presence is not considered in Ref. 17. Apart from these direct attempts to model epithermal positron transport effects, related work has also been done on epithermal positron trapping during the positron thermalization process.[18–20] Epithermal trapping can explain the positron lifetime data and the observed nonthermal positron sensitivity to near surface defects.

In this paper we will present a simple model describing both thermal and epithermal positron transport in solids; the theory is discussed in Sec. II, with discussions of the results in Sec. III, and the summary given in the last section.

II. THEORY

Our model will be based on the following assumptions.

(i) Positrons as they are described by the stopping profile are epithermal. The stopping profile used here will be an exponential. The changes in the shape of the profile will not alter any of the conclusions of this paper but will make some quantitative difference.[16] Monte Carlo simulation of positron stopping in solids has been

treated to be complete when their energies are in the range of 30 eV,[21] which does not justify the application of the thermal positron diffusion equation with the obtained stopping profile. However, at relatively higher positron incident energies, the principal part of the "stopped" positron profile will not differ very much from that of thermal positrons, as will be shown later.

(ii) The epithermal positrons will be treated only in an average sense for mathematical simplicity and a clear physical picture. All epithermal positrons are represented by a single epithermal level. They are assumed to have the same velocity and the same average elastic and inelastic scattering rates. It should be noted that the scattering rates mentioned here are not simply related to the corresponding energy-dependent mfp because of the simplified one-level approximation and also because of the nonlinearities of the thermalization rate. They correspond to the thermalization length in other situations.[6,15] For example, in thin metal film measurements,[15] the mean free path of epithermal positrons is found to be 30–35 Å, while the least length required to thermalize the hot positrons is ≈ 100 Å.

(iii) Thermal positrons will still obey the diffusion equation approach.[3] Consistent with the developed one-dimensional diffusion equation for thermal positrons, we adopt a one-dimensional steady-state equation for epithermal positrons. When positrons are stopped, they will subsequently transport as epithermal positrons, governed by the various scattering mechanisms. Those that are scattered elastically will remain as epithermal during their transport in the solid, while those that suffer an inelastic scattering event will be assumed to be fully thermalized and obey the diffusion equation for thermal positrons. Thus, the source of the epithermal positrons is the incident positrons as they are described by the implantation profile, and the source for thermal positrons is the inelastically scattered epithermal positrons. Thermalization is simply represented by the inelastic scattering of epithermal positrons. The inelastic scattering could be due to electronic collision, phonon scattering, etc. The order of magnitude of the thermalization time is ≈ 10 ps, which makes the use of a steady-state equation acceptable.

The treatment of the one-dimensional epithermal positron transport developed here is based on the work of low-energy electron transport in solids.[22–25] If the positron current is $I_e(\theta,x)$ (θ is the scattering angle), and $\gamma_{\rm el},\gamma_{\rm in}$ represent the average elastic and inelastic scattering rates per unit length, $S(x)dx$ is the rate at which the positrons are being implanted between x and $x+dx$, the bulk annihilation and trapping rate per unit length is γ_a, then the equation for the current (see Ref. 25) is

$$\cos\theta\frac{dI_e(\theta,x)}{dx}=-(\gamma_{\rm el}+\gamma_{\rm in}+\gamma_a)I_e(\theta,x)+\gamma_{\rm el}\int I_e(\theta',x)\frac{dw}{4\pi}+\frac{S(x)}{4\pi}\ , \tag{1}$$

where dw is the differential angle element.

The total epithermal current $J_e(x)$ at depth x is

$$J_e(x)=\int I_e(\theta,x)\cos\theta\, dw \tag{2}$$

and the total density of epithermal positrons $n_e(x)$ at depth x is

$$n_e(x)=\frac{1}{v}\int I_e(\theta,x)dw\ , \tag{3}$$

where v is the velocity of the epithermal positrons.

Analytical solution of the integrodifferential equation (1) is in general unavailable. People have mostly adopted a two-stream approximation in which the particles are assumed moving either in the $+x$ direction or $-$x direction. Elastic scattering will result in the particle moving in one direction joining the opposite direction stream. This approach can also be generalized to any finite number streams, but here we will treat the two-stream approximation only.

Assume the average scattering angle is $\bar{\theta}$ and $\alpha=1/\cos\bar{\theta}$; then the two streams approximation gives

$$\frac{1}{\alpha}\frac{dI_+}{dx}=-\frac{\gamma_{\rm el}}{2}(I_+-I_-)-(\gamma_{\rm in}+\gamma_a)I_+ +\frac{S(x)}{4\pi}\ , \tag{4}$$

$$\frac{1}{\alpha}\frac{dI_-}{dx}=-\frac{\gamma_{\rm el}}{2}(I_+-I_-)+(\gamma_{\rm in}+\gamma_a)I_- +\frac{S(x)}{4\pi}\ , \tag{5}$$

where I_+,I_- represents the two-stream in $+$ or $-$ x directions. The flux and the density in (2) and (3) are then expressed as

$$J_e(x)=\frac{2\pi}{\alpha}(I_+-I_-)\ , \tag{6}$$

$$n_e(x)=\frac{2\pi}{v}(I_++I_-)\ . \tag{7}$$

From Eq. (4), forward moving positrons are depleted by scattering, annihilation, and trapping, while being augmented by the elastically scattered backward moving positrons; the opposite is true for the backward stream. Combining Eqs. (4) and (5) yields

$$\frac{1}{\alpha}\frac{d}{dx}(I_++I_-)=-(\gamma_{\rm el}+\gamma_{\rm in}+\gamma_a)(I_+-I_-)\ , \tag{8}$$

$$\frac{1}{\alpha}\frac{d}{dx}(I_+-I_-)=-(\gamma_{\rm in}+\gamma_a)(I_++I_-)+\frac{S(x)}{2\pi}\ . \tag{9}$$

Substituting (9) into (8) and employing at the same time the relation between I_+,I_- and n_e,J_e [(6) and (7)], we obtain a diffusion equation for the epithermal positrons:

$$\frac{v}{\alpha^2(\gamma_{\rm in}+\gamma_{\rm el}+\gamma_a)}\frac{d^2n_e(x)}{dx^2}=(\gamma_{\rm in}+\gamma_a)vn_e(x)-S(x)\ . \tag{10}$$

The corresponding flux density is

$$J_e(x)=-\frac{v}{\alpha^2(\gamma_{\rm in}+\gamma_{\rm el}+\gamma_a)}\frac{dn_e(x)}{dx} \tag{11}$$

with an effective diffusion coefficient

$$D_e=\frac{v}{\alpha^2(\gamma_{\rm el}+\gamma_{\rm in}+\gamma_a)}\ .$$

For the thermalized positrons the diffusion equation gives

$$D_t \frac{d^2 n_t(x)}{dx^2} - \lambda_{\text{eff}} n_t(x) + S'(x) = 0 , \tag{12}$$

where $S'(x) = \gamma_{\text{in}} v n_e(x)$ is the rate of thermal positrons being fed into x to $x+dx$ because of the inelastically scattered epithermal positrons, $n_t(x)$ is the density of thermalized positrons, λ_{eff} is the effective annihilation and trapping rate,[3] and D_t is the diffusion coefficient for thermal positrons.

Equation (10) indicates that epithermal positrons either diffuse back to the surface or are inelastically scattered or are trapped and annihilate with electrons. If $\gamma_{\text{in}} \gg \gamma_a$, the annihilation and trapping fraction may be neglected compared to the high inelastic scattering rate, and the diffusion behavior of epithermal positrons is then seen to be limited by frequent inelastic scattering. Thus, for distances far greater than the average inelastic mean free path l_{in} (thermalization length) from the surface, there will be a negligibly small fraction of epithermal positrons reemitted. Those epithermal positrons implanted deep inside the solid will become effectively thermalized while they are diffusing back to the surface. Equations (4)–(12) give the mathematical description of the positron thermalization and the transport of positrons before and after thermalization.

In the following we will solve Eqs. (4)–(12) by assuming a totally absorbing boundary, i.e., $n(x)|_{x=0} = 0$. The $S(x)$ is the implantation profile in a steady-state transport equation that corresponds to a time-averaged rate of feeding the epithermal positrons into the solid. We assume an exponential profile given by

$$S(x) = (1/x_0)\exp(-x/x_0) , \tag{13}$$

where $x_0 = (A/\rho)E^n$, E is the incident positron energy, ρ is the density of the material in g/cm^3, A and n are constants, [$n = 1.3$–1.8, while $A \approx 400$ Å/(keV)^n]. The Green's function for a diffusion equation similar to (10) or (12) that is defined in a semi-infinite space and has a total absorbing boundary is

$$G(x,x') = (1/2\beta D)\{\exp(-\beta|x-x'|) - \exp[-\beta(x+x')]\} , \tag{14}$$

where $1/\beta$ is the diffusion length and D is the diffusion coefficient. For epithermal positrons, Eq. (10) yields

$$n_e(x) = \frac{1}{v\gamma_{\text{in}} x_0'}(e^{-x/x_0} - e^{-\beta_e x}) , \tag{15}$$

where

$$\beta_e = \alpha\sqrt{(\gamma_{\text{in}}+\gamma_a)(\gamma_{\text{in}}+\gamma_a+\gamma_{\text{el}})} ,$$

$$x_0' = \frac{x_0^2\beta_e^2 - 1}{\alpha x_0 \beta_e \gamma_{\text{in}}}\sqrt{(\gamma_{\text{in}}+\gamma_a)/(\gamma_{\text{in}}+\gamma_a+\gamma_{\text{el}})} .$$

Thus

$$S'(x) = \gamma_{\text{in}} v n_e(x) = \frac{1}{x_0'}(e^{-x/x_0} - e^{-\beta_e x}) .$$

For thermal positrons with diffusion length $1/\beta_t$, Eq. (12) gives thermal positron density

$$n_t(x) = \frac{1}{D_t x_0'}\left[\frac{e^{-x/x_0} - e^{-\beta_t x}}{\beta_t^2 - 1/x_0^2} - \frac{e^{-\beta_e x} - e^{-\beta_t x}}{\beta_t^2 - \beta_e^2}\right] \tag{16}$$

and the total thermalized positron fraction

$$F_{\text{th}} = \int_0^\infty S'(x)dx = \frac{\alpha\gamma_{\text{in}} x_0}{1+x_0\beta_e}\sqrt{(\gamma_{\text{el}}+\gamma_{\text{in}}+\gamma_a)/(\gamma_{\text{in}}+\gamma_a)} . \tag{17}$$

The fraction of epithermal positrons that reach the surface is then

$$J_e = \frac{D_e}{v\gamma_{\text{in}} x_0'}\left[\beta_e - \frac{1}{x_0}\right] , \tag{18}$$

while the fraction of thermalized positrons that have returned to the surface is

$$J_t = \frac{1}{x_0'}\left[\frac{1}{\beta_t + 1/x_0} - \frac{1}{\beta_t+\beta_e}\right] . \tag{19}$$

The results will be discussed in Sec. III.

III. DISCUSSION

With the one-dimensional thermal positron diffusion equation approach, it is found that the fraction of thermal positrons returning to the surface is

$$F_s = \frac{1}{1+x_0\beta_t} \tag{20}$$

for an exponential implantation profile and totally absorbing boundary in a semi-infinite space. Here x_0 is defined the same as in (13).

To make a comparison with (20) we will first discuss the results obtained from our model when inelastic scattering due to phonons or electrons is dominant, and the sample is pure enough that epithermal positron trapping can be neglected. We have the following relations:

$$\gamma_{\text{in}} \gg \gamma_{\text{el}} \gg \gamma_a$$

and

$$\beta_e \approx \alpha\gamma_{\text{in}}, \quad x_0' \approx (\alpha^2 x_0^2 \gamma_{\text{in}}^2 - 1)/\alpha^2 x_0 \gamma_{\text{in}}^2 .$$

The fraction of epithermal positrons that experience inelastic scattering and become thermalized is

$$F_{\text{th}} = \frac{\alpha x_0 \gamma_{\text{in}}}{1+\alpha x_0 \gamma_{\text{in}}} . \tag{21}$$

This fraction tends to unity when inelastic scattering is dominant and when the implantation depth of the positron is much greater than the thermalization length. To some extent this justifies the use of the thermal positron diffusion equation solution with an as-implanted profile (13) when the incident energy of the positrons is very high.

The fraction of thermal positrons that returns to the surface is

$$J_t=\frac{1}{\beta_t x_0'+x_0'x_0}-\frac{1}{\beta_t x_0'+\alpha\gamma_{\rm in}x_0'} \tag{22}$$

and that of epithermal positrons is

$$J_e=\frac{1}{1+\alpha x_0\gamma_{\rm in}} \tag{23}$$

when $\alpha\gamma_{\rm in}x_0\gg 1$. It is seen that the fraction of epithermal positrons returning to the surface is proportional to E^{-n} ($n\approx 1.5$) with E the positron incident energy. Thus, it is possible to experimentally evaluate n by measuring the epithermal positron flux at the surface. Howell *et al.*[12] deduced from their experiment that the nonthermal positronium yield at the surface is proportional to E^{-1} but not E^{-n}. Apart from the simplicity of the present model and insufficient experimental accuracy, other reasons for the inconsistency may be a nonlinear branching ratio for the returned epithermal positron to pick up an electron at the surface and form positronium. It may also be true that the implantation depth at low energy is simply not a power-law relation with the incident energy of the positron. In fact, there are no results on the shape of the positron stopping profile when incident energy is below 500 eV.

The source profile for thermal positrons in this case is evaluated as

$$S'(X)=\frac{\alpha^2x_0\gamma_{\rm in}^2}{\alpha^2x_0^2\gamma_{\rm in}^2-1}(e^{-x/x_0}-e^{-\alpha\gamma_{\rm in}x}) . \tag{24}$$

This profile can be well approximated by (13) when the positrons are deeply implanted and inelastic scattering is dominant, i.e., $\alpha\gamma_{\rm in}x_0\gg 1$.

It is clearly seen by comparing (22) with (20) that the fraction of returned thermal positrons is changed when the thermalization process is considered. This effect is especially large when the implantation depth x_0 is smaller than or comparable to the average thermalization length. In Fig. 1 we have plotted (20), (22), and (23) for a thermalization length $(1/\gamma_{\rm in})\approx 100$ Å, and a diffusion length for thermal positrons ≈ 800 Å with α taken to be 2 (other figures use the same parameters). Equation (20) gives the reemitted thermal positron fraction (dashed line), which decreases monotonically with incident positron energy. Its slope is characterized by an energy corresponding to β_t. The solid line is the reemitted thermal positron fraction from our model [Eq. (22)]. It coincides with (20) at high positron incident energies, but is depleted at low incident energies because of epithermal positron reemission. The dotted line represents the reemitted epithermal positron fraction from Eq. (23). The inset of Fig. 1 is the low-energy part; it shows that the deviation of our model from the standard diffusion model starts around 3 keV. This is in agreement with the data analysis carried out by Huomo *et al.*, which emphasizes positron incident energies above 4 keV.

Figure 2 shows the ratio of reemitted epithermal positrons to total reemitted positrons. It is seen that the epithermal positron contribution decreases with increasing positron incident energy. This is to be compared with experimental data[26] for Cu. They are in general qualitative agreement. Overall quantitative agreement is unrealistic here, not only because of our simplified treatment of epithermal positrons, but also because of the inaccuracy of the experimental data, which was obtained by measuring the energy distribution of reemitted positron, and subtracting the thermal portion from it to evaluate the epithermal fraction.

Figure 3 shows the total thermalized fraction as obtained from (17). It is in general agreement with the

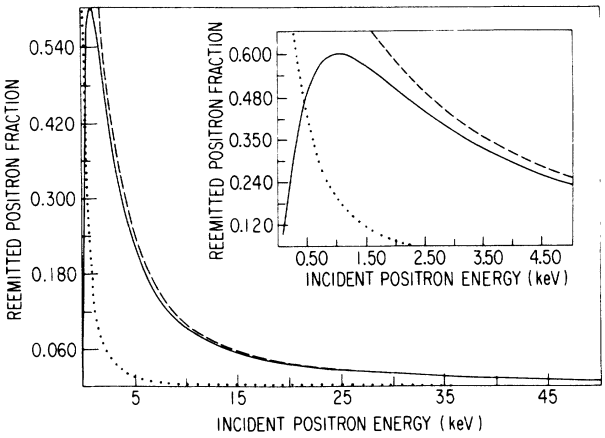

FIG. 1. Plots shown for the reemitted thermal positron fraction from the simple diffusion model [dashed line—Eq. (20)] and from the present model [solid line—Eq. (22)]. The dotted line is the reemitted epithermal positron fraction [Eq. (23)]. The inset is the enlarged view of the low-energy part.

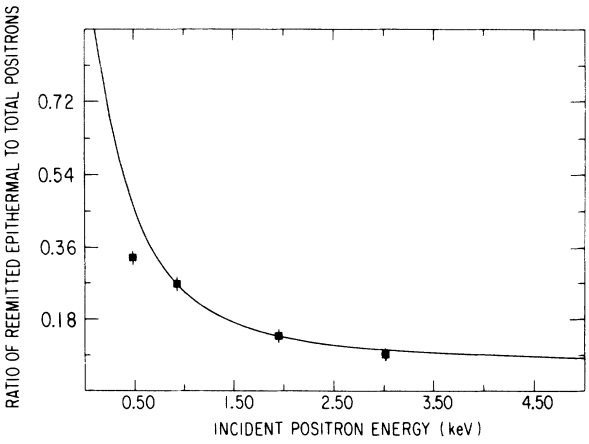

FIG. 2. Shows the ratio of reemitted epithermal positrons to total reemitted positrons as a function of incident positron energy. Experimental results for the ratio of reemitted epithermal positrons to the total positrons reemitted from a Cu(111) surface are also shown (Ref. 26).

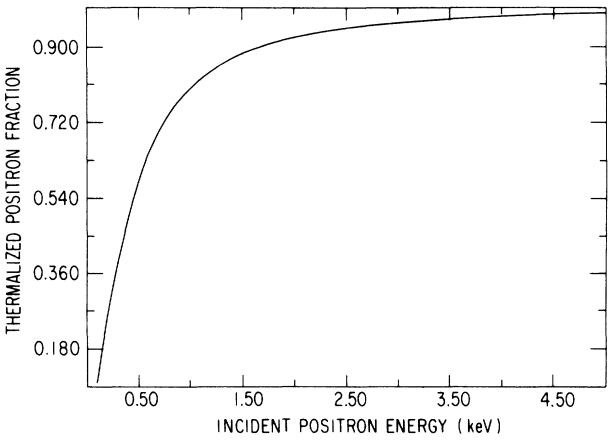

FIG. 3. Total thermalized fraction of the implanted positrons as a function of incident positron beam energy [Eq. (21)].

above discussion, and more clearly indicates the non-negligibility of epithermal positrons below ≈ 3 keV.

Apart from the positron incident energy dependence of epithermal positrons discussed previously, the change of other experimental geometries or material properties may also induce substantial contributions from epithermal positrons. Since the effective thermalization depends on the material properties such as the band gap, the electron gas density for a metal, and the available energy loss mechanisms for thermalization (e.g., the absence of optical phonon branches in materials with one atom per unit cell will make the thermalization length longer), there will certainly be differences in the parameters γ_{in}, γ_{el}, etc., for different materials.

For example, in ionic and rare-gas solids,[12,13] the incident positrons rapidly lose energy by means of electron-hole creation and Ps formation, but below the threshold for Ps formation, the only available inelastic channel is phonon scattering. The relatively high initial stopping energy caused by the lack of effective energy loss channels enables the epithermal positrons to have a large diffusion length (which can in some cases be larger than the thermal positron diffusion length limited by annihilation), and the reemission of epithermal positrons can dominate even at high positron incident energy. The use of our model for fitting the variable energy positron beam experimental results will be helpful in evaluating some energy loss as well as material dependent information. The low-energy contribution should be especially sensitive to these kinds of properties because of the above discussed epithermal positron effects at low incident positron energies for most materials, but epithermal positrons effects at high incident positron energies cannot be neglected.

The other important case is when the trapping rate becomes high enough that it is comparable to or even larger than the inelastic scattering rate.[11,18] Then the bulk annihilation (mostly due to trapping) is not negligible. The trapping of epithermal positrons has been discussed at length in Ref. 18. It is found that trapping before thermalization can be a significant part of the total trapping. In this case the annihilation line-shape S parameter can be written as

$$S = F_{ep}(S_{es}F_{es} + S_{ed}S_{ed}) + F_{\text{th}}(S_{ts}F_{ts} + S_{td}F_{td} + S_{tb}F_{tb}) , \tag{25}$$

where e represents the epithermal part, t the thermal part, and s, d, and b represent, respectively, the surface trapping, defect trapping and bulk annihilation in the free state. S is the annihilation line-shape parameter, and F is the corresponding fraction. Annihilation of free bulk epithermal positrons are neglected here because they are likely to be insignificant in all materials compared to either the inelastic scattering or the trapping rates. The effect of epithermal trapping on F-parameter measurements is that β_e and x_0' will be dependent on the trapping rate, affecting the thermalized positron fraction as well as the fraction returning to the surface, as can be seen from Eqs. (17)–(19).

IV. SUMMARY

We have treated epithermal and thermal positron transport in solids with a simple three-step model, i.e., implantation, thermalization, and diffusion, which is more complete than the previously used implantation-diffusion two-step model. The epithermal positron contribution to the F parameter is discussed. It is found that when inelastic scattering is dominant over elastic scattering and bulk trapping, the thermal positron diffusion equation approach is a good approximation at high positron incident energies. Otherwise, the effects of epithermal positrons have to be examined before any quantitative conclusions can be made. Similar results can also be obtained for the positron annihilation line-shape S-parameter measurement from our model. Future experimental work is expected to yield more precise information on both thermal and epithermal positrons for comparison with the developed model. The use of epithermal positrons in studying solids as presented in Ref. 11, when combined with a proper model description, will yield important information on material surface and near-surface studies. Variable energy positron beams are superior to the presently available electron methods in this respect because in many materials, positrons will have a small positive or even negative work function.[1] These characteristics allow positrons down to thermal energies to be reemitted spontaneously. Studies of epithermal positron effects in multilayered structures will also give more information, which would otherwise be unavailable.

However, it should be noted that the present model is unable to obtain the energy distributions of the epithermal positrons because of the single level assumed for the epithermal positrons. Current work is being done to correct this, and some results will be presented later.[16] The other point that has to be noted is that the temperature dependence of the properties of the scattering mech-

anisms for epithermal positrons have to be understood before the model can be further applied to the temperature dependence of experimental data. There has been some theoretical work in this respect.[6] Experimentally, positron reemission from thin metal films will provide a direct means to measure the mean free path and its temperature dependence, thermalization rates, etc.[15] The present model itself will help extract new information on the temperature properties of the epithermal positrons from such experiments.

ACKNOWLEDGMENTS

We wish to thank Dr. J. Throwe and Dr. A. B. Walker for careful readings of the manuscript, and Dr. B. Nielsen and E. Gramsch for useful discussions, we are also grateful to Professor L. Roellig for his help during the course of this work. Work was supported in part by the U.S. Department of Energy, Division of Material Science, Contract No. DE-AC02-76CH00016, and the National Science Foundation, Grant No. DMR-8315691.

---

*Also at City College, CUNY, New York, N.Y. 10031.

[1]P. J. Schultz and K. G. Lynn, Rev. Mod. Phys. **60**, 701 (1988).

[2]A. Valkealahti and R. M. Nieminen, Appl. Phys. A **35**, 51 (1984).

[3]K. G. Lynn, in *Positron Solid State Physics,* edited by W. Brandt and A. Dupasquier (North-Holland, Amsterdam, 1983).

[4]P. J. Schultz, K. G. Lynn, and B. Nielsen, Phys. Rev. B **32**, 1369 (1985).

[5]H. Huomo, A. Vehanen, M. D. Bentzon, and P. Hautojarvi, Phys. Rev. B **35**, 8252 (1987).

[6]R. M. Nieminen and J. Oliva, Phys. Rev. B **26**, 2226 (1980).

[7]K. G. Lynn, P. J. Schultz, and I. K. Mackenzie, Solid State Commun. **38**, 473 (1981).

[8]P. J. Schultz and K. G. Lynn, Phys. Rev. B **26**, 2390 (1982).

[9]D. T. Britton, P. A. Huttunen, J. Makinen, E. Soininen, and A. Vehanen, Phys. Rev. Lett. **62**, 2413 (1989).

[10]R. J. Wilson, Phys. Rev. B **27**, 6974 (1983).

[11]B. Nielsen, K. G. Lynn, and Y. C. Chen, Phys. Rev. Lett. **57**, 1789 (1986).

[12]A. P. Mills, Jr. and W. S. Crane, Phys. Rev. Lett. **53**, 2165 (1984).

[13]E. M. Gullikson and A. P. Mills, Jr., Phys. Rev. Lett. **57**, 376 (1986).

[14]R. Howell, I. J. Rosenberg, and M. J. Fluss, Phys. Rev. B **34**, 3069 (1986).

[15]D. W. Gidley and W. E. Frieze, Phys. Rev. Lett. **60**, 1193 (1988).

[16]Y. Kong and K. G. Lynn, following paper, Phys. Rev. B **41**, 6185 (1990).

[17]D. T. Britton, P. C. Rice-Evans, and J. H. Evans, Philos. Mag. Lett. **57**, 165 (1988).

[18]K. G. Lynn, T. McKay, and B. Nielsen, Phys. Rev. B **36**, 7107 (1987).

[19]W. K. Warburton and M. A. Shulman, Phys. Lett. **60A**, 448 (1977).

[20]W. Luhr-Tanck, Th. Kurschat, and Th. Hohenkamp, Phys. Rev. B **31**, 6994 (1985).

[21]K. G. Lynn and M. McKeown (private communication).

[22]J. Bernasconi, E. Cartier, and P. Pfluger, Phys. Rev. B **38**, 12 567 (1988).

[23]G. Bader, G. Perluzzo, L. G. Caron, and L. Sanche, Phys. Rev. B **26**, 6019 (1982).

[24]P. J. Chantry, A. V. Phelps, and G. J. Schultz, Phys. Rev. **152**, 81 (1966).

[25]S. Chandrasekhar, *Radiative Transfer* (Clarendon, Oxford, England, 1950).

[26]D. Fischer *et al.* (unpublished results).